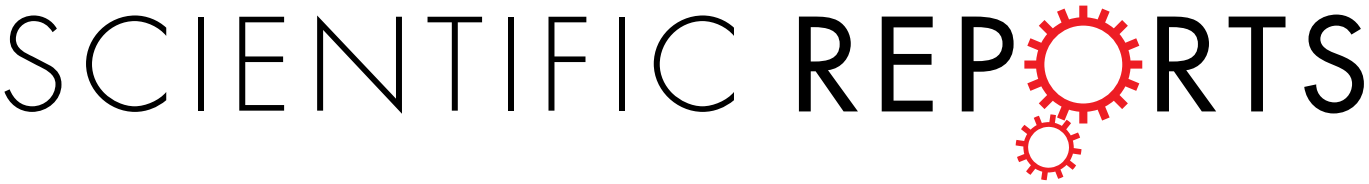

OPEN

Cuprous halides semiconductors as a new means for highly efficient light-emitting diodes

Received: 16 September 2015
Accepted: 11 January 2016
Published: 16 February 2016

Doyeol Ahn[1,2] & Seoung-Hwan Park[3]

In group-III nitrides in use for white light-emitting diodes (LEDs), optical gain, measure of luminous efficiency, is very low owing to the built-in electrostatic fields, low exciton binding energy, and high-density misfit dislocations due to lattice-mismatched substrates. Cuprous halides I-VII semiconductors, on the other hand, have negligible built-in field, large exciton binding energies and close lattice matched to silicon substrates. Recent experimental studies have shown that the luminescence of I-VII CuCl grown on Si is three orders larger than that of GaN at room temperature. Here we report yet unexplored potential of cuprous halides systems by investigating the optical gain of CuCl/CuI quantum wells. It is found that the optical gain and the luminescence are much larger than that of group III-nitrides due to large exciton binding energy and vanishing electrostatic fields. We expect that these findings will open up the way toward highly efficient cuprous halides based LEDs compatible to Si technology.

Most of the research on white LEDs has been focused on the group-III nitride semiconductor based devices. However, it is well known[1–6] that these devices employing nitride semiconductor quantum wells (QWs) show very low optical gain when compared with other III-V semiconductors such as GaAs due to the large built-in electrostatic fields on the order of MV/cm arising from the piezoelectric effects and the spontaneous polarizations. Also the large lattice mismatch between the nitride semiconductor and the substrates, typically, sapphire or SiC, leads to the generation of high density of misfit dislocations on the order of $10^{10}\,cm^{-2}$ which would also degrade the performances and the longevity of the device. In order to reduce the internal fields, an approach using the III-V wurtzite phase grown on non-polar or semi-polar substrates has been proposed[7–13]. However, layers grown on these non-polar or semi-polar substrates contain high density of non-radiative recombination centers, which have deleterious effects as well[13]. Another wide band-gap semiconductors such as II-VI ZnO has an energy band-gap of 3.3 eV at room temperature and an exciton binding energy of 63 meV[14–18]. For comparison, the exciton binding energy of GaN is 20 meV. The exciton binding energy is regarded as a measure of the interaction between electrons and holes and may be used to predict the strength of electron-hole recombination processes which are related to quantum efficiencies of the light emitting devices[19]. Therefore, wide band-gap II-VI ZnO quantum well (QW) structures have attracted much attention[14–16]. Unfortunately, it has proven difficult for ZnO semiconductor to achieve high p-type doping which is essential for the device implementation[17].

Recently, I-VII γ-cuprous halides semiconductors[20] such as CuCl, CuBr, and CuI have drawn attention[21–44] because these are zincblende direct band-gap semiconductors (3.3 eV for CuCl, 2.91 eV for CuBr and 2.95 eV for CuI) and have large exciton binding energies (190 meV for CuCl, 108 meV for CuBr and 58 meV for CuI) with their lattice constants closely matched to that of Si as can be seen by the table 1. From this table, one can see that the lattice constant of Si, 0.543 nm, is very closely matched to that of CuCl, 0.542 nm. The cuprous halides atoms form tetrahedraly coordinated helides isomorphic with the diamond-crystal fcc lattice such as Si[45]. The zinc-blende structure of cuprous halides semiconductors consists of two interpenetrating fcc lattices displaced along a body diagonal. On one fcc lattice, the Cu atoms are located and on the other side the atoms are halogen type (Fig. 1). On top of that, these cuprous halides are transparent p-type in its natural states due to the presence of Cu vacancies resulting from excess halogen[42–44]. It is also shown[37] that the incorporation of Zn by co-evaporation of

[1]Department of Electrical and Computer Engineering and Center for Quantum Information Processing, University of Seoul, Seoul 130-743, Republic of Korea. [2]Peta Lux Inc., 3F, TLi Building, 12 Yanghyeon-ro, 405 beon-gil, Jungwon-gu, Seongnam-si, Gyeonggi-do 462-100, Republic of Korea. [3]Electronics Department, Catholic University of Daegu, Hayang, Kyeongbuk 712-702, Republic of Korea. Correspondence and requests for materials should be addressed to D.A. (email: dahn@uos.ac.kr).

	CuCl	CuBr	CuI
$E_g(eV)$	3.399	2.91	2.95
$m_c(\Gamma_{6C})/m_0$	0.5	0.21	0.3
$m_p(\Gamma_{7V})/m_0$	2.0	1.6	2.43
Lattice constant (nm)	0.54202	0.56897	0.60521
$C_{11}(10^{11}\ dyn\ cm^{-2})$	0.47	0.458	0.451
$C_{12}(10^{11}\ dyn\ cm^{-2})$	0.362	0.354	0.307
$C_{44}^{E}(10^{11}\ dyn\ cm^{-2})$	0.145	0.139	0.182
$C_{44}^{D}(10^{11}\ dyn\ cm^{-2})$	0.162	–	0.185
$b(eV)$	−0.7	−0.4	–
$\varepsilon(\infty)$	7.9	4.062	4.58
$\Delta_{so}(meV)$	−40.4	150	640
Exciton binding energy (meV)	190	108	58

Table 1. Material parameters of cuprous halides semiconductors (ref. 45).

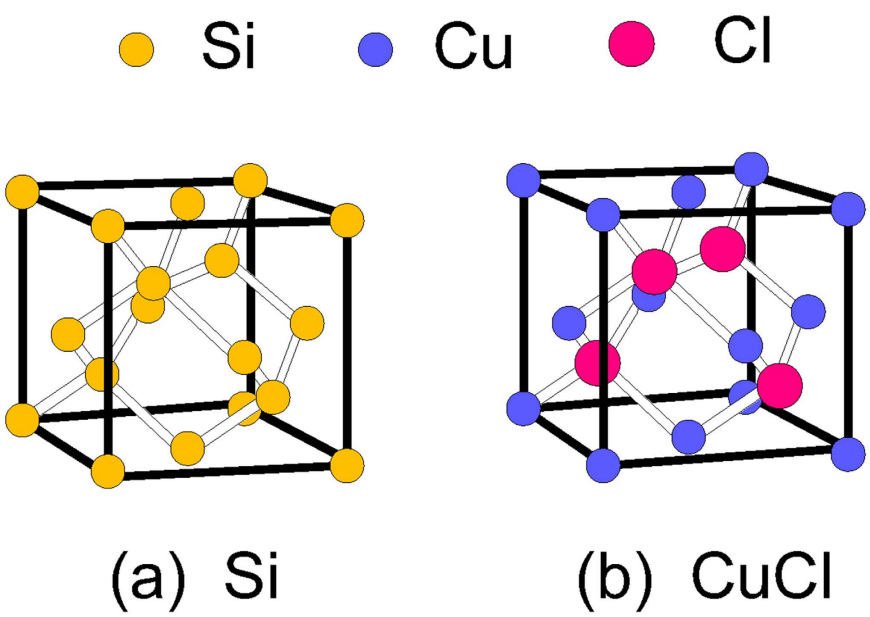

Figure 1. (**a**) The diamond-crystal fcc lattice characterized by four covalent bonded Si atoms. (**b**) The zincblende fcc lattice of cuprous halides crystals such as CuCl, CuBr and CuI. The zincblende structure consists of two interpenetrating fcc lattices displaced along a body diagonal. On one fcc lattice, the atoms are Cu and on the other side they are halogen atoms.

CuCl and $ZnCl_2$ yields n-type doping. The piezoelectric stress coefficient e_{14} for CuI is $1.27 \times 10^{-5} C/cm^2$ which is lower than that of GaAs, $1.6 \times 10^{-5} C/cm^2$ [45,46]. Since the piezoelectric effects of GaAs is much smaller than that of GaN or InGaN, we can ignore the piezoelectric field effects for CuI/CuCl QWs[47]. The spontaneous polarization arises from the intrinsic asymmetry of the bonding of wurtzite crystal structure[47]. Therefore, in the zincblende structure, the spontaneous polarization would be negligible.

Researches on the cuprous halides semiconductors have been focused on the following areas over the past decade: (1) spectroscopic and theoretical studies of band structures[26–33], (2) photoluminescence studies of I-VII quantum dots embedded in NaCl crystals and glasses[22,24,25,33], (3) surface studies of the growth mechanisms involved in the hetero epitaxy, and single crystal and poly crystal layer growth on Si and GaAs[23,35–40]. Especially, Nishida *et al.*[23] demonstrated single crystal thin layera growth on GaAs and Si using ultra high vacuum (UHV) molecular beam epitaxy (MBE). As for a direct evidence of the exciton binding energy effects on the luminescence, it was observed that the luminescence of liquid phase epitaxy (LPE) grown polycrystalline CuCl on Si is considerably brighter (by 3 order of magnitude) than undoped single crystal GaN grown sapphire at room temperature[39]. An electroluminescence (EL) device employing polycrystalline γ-CuBr thin film active layer was also demonstrated[40]. However, there has been very little work on device physics studies of these I-VII semiconductors, considering their potential impacts on the high efficient light-emitting devices.

In this article, we report the theoretical study of an optical gain and the luminescence of I-VII CuI/CuCl quantum well structures on Si substrates in high efficiency light-emitting device for the first time. A multi-band

effective mass approach[48–51] and non-Markovian optical gain model including the excitonic effects are employed[52,53]. The Luttinger parameters of zincblende I-VII cuprous halides semiconductors, necessary for the band-structure calculation, are obtained from a semi-empirical five level $\vec{k}\cdot\vec{p}$ approach[41,48,49]. It is observed that the optical gain and the luminescence of cuprous halides CuI/CuCl and CuBr/CuCl QWs would be much higher than those of III-V nitride layers or II-VI ZnO/MgZnO QWs due to the inherent strong excitonic effects and negligible electrostatic fields within the active layers. Our predictions agree with recent experimental results[39] qualitatively. Substantially high optical gain of I-VII cuprous halides QWs as compared with that of III-V nitride QWs or II-VI ZnO QWs and the cuprous halides semiconductor structure's close lattice match to Si substrate are the clear manifestation of the possibility of highly efficient I-VII cuprous halides semiconductor based light-emitting devices for solid-state lighting and integrated optoelectronic components compatible to Si technology. This study is also expected to suggest further work on the device implementation of I-VII semiconductors.

Results

We first obtain the Luttinger parameters of zincblende CuI and CuCl from a semi-empirical five level $\vec{k}\cdot\vec{p}$ approach including d electron effects[41,48,49]. The band structure of a CuI/CuCl quantum well is calculated within the 6×6 multiband effective mass theory which also takes into account the biaxial strain, spontaneous polarization and the piezoelectric effects[13,41]. To calculate the optical gain, we used non-Markovian model based on time-convolutionless reduced-density operator formalism which includes the many-body effects such as the band-gap renormalization, enhancement of optical gain due to attractive electron-hole interaction called excitonic effects, and the plasma screening[52,53]. The mean field Coulomb effect is included in the interband reduced-density operator which gives the complete exciton effects with all bound states. Excitonic effects are particularly important for CuI and CuCl, which show the photoluminescence dominated by, $Z_{1,2}$ and Z_3 excitonic states in moderate carrier densities. In our model, the optical gain is given by[52,53]

$$g(\omega) = \frac{\omega\mu c}{n_r}\frac{1}{V}Tr\ \mathrm{Re}\left\{\frac{\Xi(0,\Delta_k)}{1-q_k(0)}|\mu(k)|^2[1+g_2(\infty,\Delta_k)][n_{ck}^0-n_{vk}^0]\right\}, \tag{1}$$

with

$$q_k(0) = i\Xi(0,\Delta_k)\mu^*(k)\left[[n_{ck}^0-n_{vk}^0]\sum_{k'}\frac{V_s(k'-k)}{\mu^*(k')}\right]. \tag{2}$$

Here, μ is the permeability, n_r is the refractive index, c is the speed of light in free space, V is the volume, Tr denotes the trace, $\Xi(0,\Delta_k)$ is the lineshape function that describes the spectral shape of the optical gain in driven semiconductor, $\mu(k)$ is the dipole moment, n_{ck}^0 and n_{vk}^0 is the quasi-equilibrium distributions of electrons in the conduction band and valence band, respectively, k is the wave vector, $V_s(k)$ is screened Coulomb potential, ω is the angular frequency of the optical field, g_2 is the optical phase detuning and $\Delta_k = E_c^{sc}(k) - E_v^{sc}(k) - \hbar\omega$, where $E_c^{sc}(k)$ and $E_v^{sc}(k)$ are renormalized energies of electrons in the conduction band and valence band, respectively.

In equation (1), the factor $1/(1-q_k(0))$ describes the excitonic enhancement factor where the vertex function $q_k(0)$ is exact in the steady-state approximation and is equivalent to the one derived from the solution of the Bether-Salpeter equation obtained from the many-body Green's function approach[52]. The excitonic effects are all contained in the vertex function $q_k(0)$.

Band-structure. The results of our valence-subband calculation are shown in Fig. 2 for a 30 Å CuI/CuCl quantum-well versus in-plane wave vector in unit of $2\pi/a_0$ where a_0 is the lattice constant of CuI. We have used 6×6 Luttinger-Kohn model taking into account of the biaxial compressive strain due to the lattice mismatch between CuI and CuCl. We assume that the band-gap discontinuity of CuI/CuCl quantum well is evenly distributed between the conduction band and the valence band. One must note that the spin-orbit (SO) band belong to Γ_7 lies 40.4 meV above the Γ_8 band in the case of CuCl but the SO band is below 640 meV from Γ_8 band in the case of CuI at the Brillouin zone center[26]. As a result, the contribution of the SO band on the band mixing of heavy- and light-hole subbands would be negligible. In this figure, HH1 denotes the first state of the heavy hole (HH) subband and LH1 is the first state of light hole subbands.

Optical gain and luminescence with excitonic enhancement. From equation (1), it is evident that the integrand for the optical gain would be strongly affected by the excitonic enhancement factor $1/(1-q_k(0))$. In Fig. 3, we show the $\mathrm{Re}q_k(0)$ between the ground states of conduction and valence bands for CuI/CuCl QW (red), CuBr/CuCl QW[41] (blue), ZnO/$Mg_{0.3}Zn_{0.7}O$ QW (green), and $In_{0.2}Ga_{0.8}N/Al_{0.2}In_{0.005}Ga_{0.7995}N$ QW (black). The carrier density of $3\times 10^{19}\,cm^{-3}$, intraband relaxation time of 10 fs and the correlation time of 25 fs are assumed in the calculation[41]. In the cases of II-VI and III-V nitride QWs, the band structure of the hexagonal crystalline lattice is taken into account[13]. It is seen that the $\mathrm{Re}q_k(0)$ for CuI/CuCl QW and CuBr/CuCl QW are much larger than that of InGaN/AlInGaN QW in magnitude when compared as functions of the in-plane wave vector. In all four cases, however, we have that $\mathrm{Re}q_k(0)<1$. Since the Coulomb enhancement factor is inversely proportional to $1-\mathrm{Re}q_k(0)$, the excitonic effects on the optical gain would be appreciable for I-VII QWs as can be seen in this figure. From this result, it is predicted that the enhancement of gain would be most pronounced in the case of I-VII QW then followed by II-VI ZnO/MgZnO QW. The strong excitonic effects manifested by $\mathrm{Re}q_k(0)$ in Fig. 2 agree at least qualitatively with the experimental results[32–34].

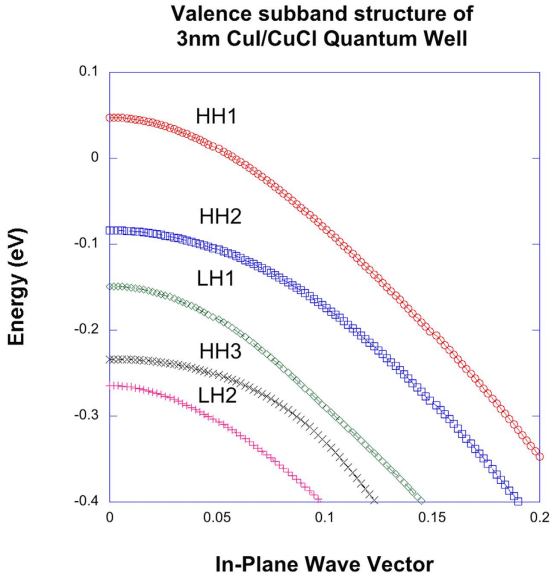

Figure 2. Valence-subband structure of a 30 Å CuI/CuCl quantum-well versus in-plane wave vector in unit of $2\pi/a_0$ where a_0 is the lattice constant of CuI. We have used 6 × 6 Luttinger-Kohn model taking into account of the biaxial compressive strain due to the lattice mismatch between CuI/CuCl.

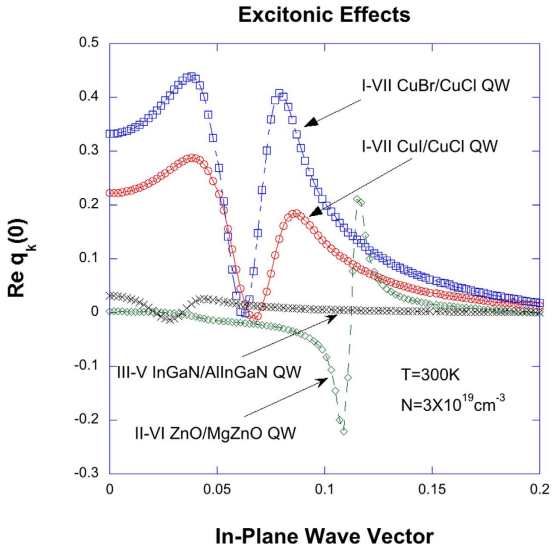

Figure 3. Req_k(0) between the ground states of conduction and valence bands for CuI/CuCl QW (red), CuBr/CuCl QW (blue), ZnO/$Mg_{0.3}Zn_{0.7}O$ QW (green), and $In_{0.2}Ga_{0.8}N/Al_{0.2}In_{0.005}Ga_{0.7995}N$ QW (black). The carrier density of $3 \times 10^{19}\,cm^{-3}$, intraband relaxation time of 10 fs and the correlation time of 25 fs are assumed in the calculation. In the cases of II-VI and III-V nitride QWs, the band structure of the hexagonal crystalline lattice is taken into account[13].

In Fig. 4, non-Markovian optical gain spectra with Coulomb or excitonic enhancement are plotted for CuI/CuCl QW (red), CuBr/CuCl QW (blue), ZnO/$Mg_{0.3}Zn_{0.7}O$ QW (green), and $In_{0.2}Ga_{0.8}N/Al_{0.2}In_{0.005}Ga_{0.7995}N$ QW (black) versus photon energy for carrier density of $5 \times 10^{19}\,cm^{-3}$. Band-gap renormalization is taken into account in all cases. From Figs 3 and 4, we expect that the many-body effects, especially, the Coulomb effects are becoming more important in the case of cuprous halides I-VII QWs whose peak gain is an order of larger than that of InGaN-AlInGaN QW. The optical gain of II-VI ZnO/MgZnO QW is still larger than that of InGaN-AlInGaN QW but ZnO cannot be grown on Si because of too much lattice mismatch unlike the case of I-VII QWs and p-type doping is difficult. I-VII CuI and CuBr are known to have similar effective masses as GaN at the zone center[35], so the main reason of much larger gain of the cuprous halides semiconductor is the large diploe matrix elements which is almost an order of magnitude larger than that of nitride semiconductors as can be seen in Fig. 5 and the excitonic effects shown in Fig. 3.

The dipole moment $\mu_{lm}^{\eta\sigma}(\vec{k}_{\|})$ is defined by[52]

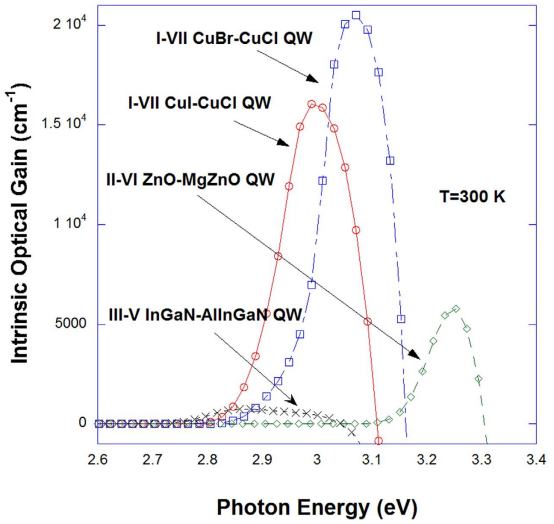

Figure 4. on-Markovian optical gain spectra with Coulomb or excitonic enhancement are plotted for CuI/CuCl QW (red), CuBr/CuCl QW (blue), ZnO/$Mg_{0.3}Zn_{0.7}O$ QW (green), and $In_{0.2}Ga_{0.8}N/Al_{0.2}In_{0.005}Ga_{0.7995}N$ QW (black) versus photon energy for carrier density of $5 \times 10^{19}\, cm^{-3}$. Band-gap renormalization is taken into account in all cases. In the cases of II-VI and III-V nitride QWs, the band structure of the hexagonal crystalline lattice is taken into account[13].

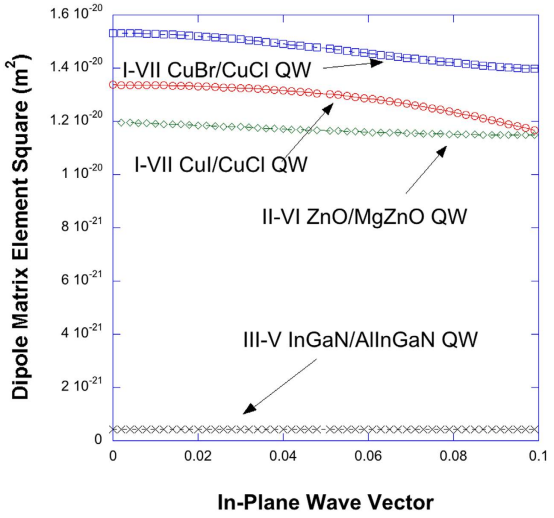

Figure 5. Dipole matrix element squares are plotted for CuI/CuCl QW (red), CuBr/CuCl QW (blue), ZnO/$Mg_{0.3}Zn_{0.7}O$ QW (green), and $In_{0.2}Ga_{0.8}N/Al_{0.2}In_{0.005}Ga_{0.7995}N$ QW (black) versus photon energy. In the cases of II-VI and III-V nitride QWs, the band structure of the hexagonal crystalline lattice is taken into account (ref. 13).

$$\mu_{lm}^{\eta\sigma}(\vec{k}_{\|}) = \begin{cases} \sum_{\nu=1,2,3} \langle g_m^{(\nu)} | \phi_l \rangle \langle \nu | \hat{\varepsilon} \cdot e\vec{r} | S, \eta \rangle \text{ for } \sigma = U \\ \sum_{\nu=4,5,6} \langle g_m^{(\nu)} | \phi_l \rangle \langle \nu | \hat{\varepsilon} \cdot e\vec{r} | S, \eta \rangle \text{ for } \sigma = L \end{cases}, \tag{3}$$

where $g_m^{(\nu)}(\vec{k}_{\|}, z)$ is the hole envelope function; $\{|\nu\rangle\}$ denotes the transformed Bloch basis at the zone center; m is the quantum well subband index; $\vec{k}_{\|} = k_x\hat{x} + k_y\hat{y}$, $\vec{r}_{\|} = x\hat{x} + y\hat{y}$ and $\sigma = U$(or L) refers to the upper (or lower) blocks; respectively; $\phi_l(z)$ is the electron envelope function for the lth conduction subband with a spin state η; and $\hat{\varepsilon}$ is the unit vector in the direction of the photon polarization.

From equation (3), it is straightforward to see that the dipole moment is proportional to the overlap integral of electron and hole wave functions. In Fig. 6, normalized ground state electron wave functions (blue) and the hole wave functions (red) at the zone center are plotted together with the conduction and valence band QW potential

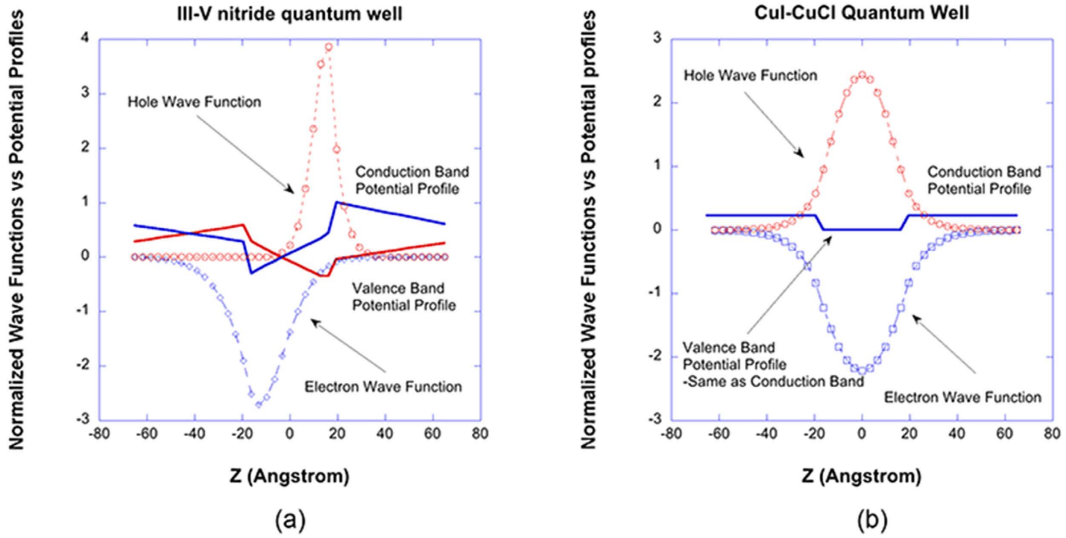

Figure 6. Normalized ground state electron wave functions (blue) and the hole wave functions (red) at the zone center are plotted together with the conduction and valence band QW potential profiles for (**a**) $In_{0.2}Ga_{0.8}N/Al_{0.2}In_{0.005}Ga_{0.7995}N$ QW and (**b**) CuI/CuCl QW.

profiles[54] for (a) $In_{0.2}Ga_{0.8}N/Al_{0.2}In_{0.005}Ga_{0.7995}N$ QW and (b) CuI/CuCl QW. In the case of III-V nitride QW, the built-in electrostatic fields cause the electron wave function and the hole wave function shifted to the opposite side of the QW, thus reducing the overlap integral in equation (3) significantly. The vertex function $q_k(0)$ for the excitonic can be approximated as[52]

$$\mathrm{Re}\, q_k(0) \approx -\sum_{k'} V_s(k-k')\,\mathrm{Im}\,\Xi(0,\Delta_k)[n^0_{ck'} - n^0_{vk'}]. \tag{4}$$

where the screened Coulomb potential $V_s(k)$ is given by[52]

$$V^{eh\sigma}_{slmml}(k) = \sum_{\nu}\int dz_1 dz_2\, |\phi_l(z_1)|^2 g^{(\nu)}_m(k', z_2)\frac{e^2}{2\varepsilon_s|k+k'|}\exp(-k|z_1-z_2|)g^{(\nu)}_m(k+k', z_2). \tag{5}$$

From equation (5), one can see that the excitonic enhancement is also strongly dependent on the overlap between the electron and hole wave functions.

From the LED device point of view, one needs to convert the optical gain into the luminescence[55–58] which describes the radiative recombination rate under equilibrium and non-equilibrium conditions. The luminesce is described by the spontaneous emission rate $R_{sp}(\omega)$, the number of emitted photons per second per unit volume per unit energy interval, is related to the optical gain $g(\omega)$ by[56–58]

$$g(\omega) = \hbar\left(\frac{\pi c}{n_r\omega}\right)^2\left\{1-\exp\left(\frac{\hbar\omega-\Delta\mu}{k_BT}\right)\right\}R_{sp}(\omega). \tag{6}$$

where $\Delta\mu = E_G + \Delta E_{SX} + \Delta E_{CH} + \mu_n - \mu_p$; μ_n and μ_p are renormalized chemical potentials for the electron and the hole, respectively, such that $g(\Delta\mu) = 0$; k_B is the Boltzmann constant; and T is the temperature. We note that at $\hbar\omega = \Delta\mu$, the definition of $R_{sp}(\omega)$ breaks down, so we interpolated $R_{sp}(\omega)$ at $\omega_{trans} = \Delta\mu/\hbar$ from the values of $R_{sp}(\omega)$ at $\omega_{trans} \pm \delta$. The importance of using the non-Markovian lineshape functions would be pronounced in the above relation between the spontaneous emission rate and the optical gain. One of the remarkable feature of this relation is that there is a transparency point in the gain spectra which coincide with the chemical potential separation that suggests the carriers and the photons are in equilibrium or in quasi-equilibrium[57]. The optical gain spectra calculated with the Lorentzian line shape function have two errors: unnatural absorption region below the renormalized bandgap energy and mismatch of the transparency point of the gain with the chemical potential separation. It was shown in the previous work[57], that these two anomalies associated with the Lorentzian lineshape are removed in the non-Markovian model with many-body effects. In Fig. 7, the luminescence spectra calculated by equation (5) are plotted for CuI/CuCl QW (red) and $In_{0.2}Ga_{0.8}N/Al_{0.2}In_{0.025}Ga_{0.7975}N$ QW (blue) versus photon energy for the carrier density of $3\times10^{19}\,cm^{-3}$. From Fig. 7, it is expected that an order of magnitude increase for cuprous halides as compared with group III-nitride quantum wells. The efficiency of the luminescence for LEDs would depend on the competition of radiative and non-radiative processes and detailed analysis of quantum efficiency of cuprous halides based LEDs would need further study. In Fig. 8, both optical gain and luminescen spectra for CuI-CuCl QW are calculated for different carrier densities.

In this work, we focused on cuprous haldes especially, CuI-CuCl system. There are also transition metal halides such as $ZnCl_2$. In cuprous halides, the loosely bound s electrons of the Cu atom is mostly transferred to the

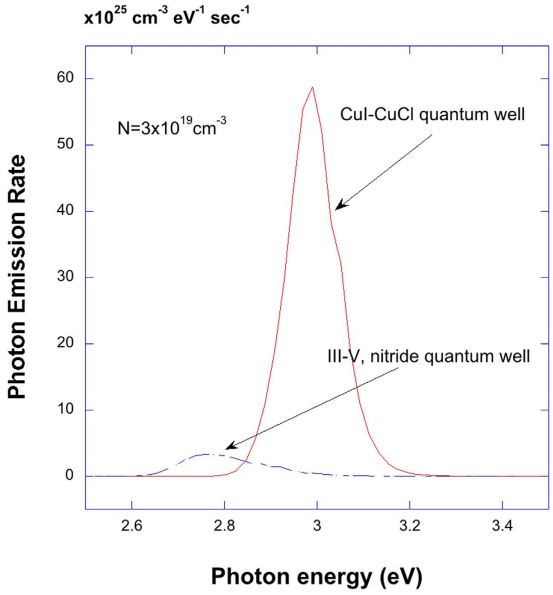

Figure 7. Luminescence spectra which gives the photon emission rate are plotted for CuI/CuCl QW (red) and $In_{0.2}Ga_{0.8}N/Al_{0.2}In_{0.025}Ga_{0.7975}N$ QW (blue) versus photon energy for the carrier density of $3 \times 10^{19}\, cm^{-3}$. The luminescence is described modified van Roosbroeck-Shockley model[52,53,55].

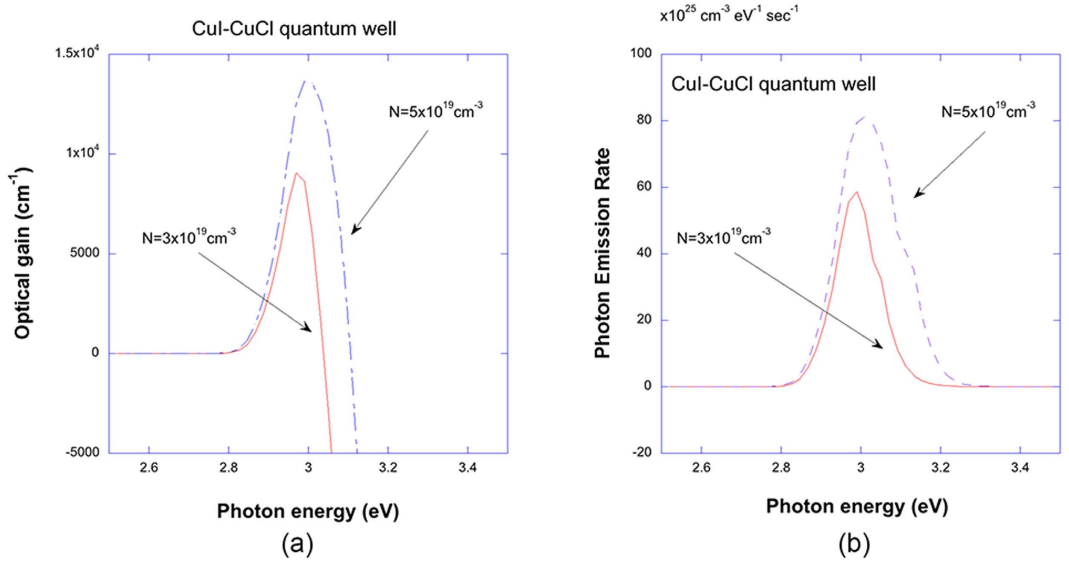

Figure 8. (**a**) Non-Markovian optical gain spectra with Coulomb or excitonic enhancement are plotted for CuI/CuCl QW versus photon energy for carrier densities of $3 \times 10^{19}\, cm^{-3}$ (red) and $5 \times 10^{19}\, cm^{-3}$ (blue). (**b**) Non-Markovian lumiescence spectra with Coulomb or excitonic enhancement are plotted for CuI/CuCl QW versus photon energy for carrier densities of $3 \times 10^{19}\, cm^{-3}$ (red) and $5 \times 10^{19}\, cm^{-3}$ (blue).

more electronegative halogen[59]. This leaves the Cu ion with completely filled outer d shell and the halogen ion with the rare-earth configuration. Unlike the I-VII alkali halides in which the d shell are core-like, the spatial extent of the d level is large and their energies are close to those of the p levels of the halogen[59]. On the other hand, most transition metal has partially filled d shells except Zn which has complexly filled d shell with the electronic configuration of $d^{10}s^2$. If the d shell of Zn ion is not core-like and the comparable to p level energies of the halogen atom, then its behaviour may be similar to that of cuprous halides. Otherwise, electronic as well as optical properties would be different.

It would require further work to compare the cuprous halides and transition metal halides.

Discussions

Built-in electrostatic fields in the active layer of the group-III nitrides LEDs have deleterious effects on the luminous efficiencies[1–6]. It is also found that the use of lattice-mismatched substrates cause the generation of

high-density misfit-dislocations that affect the longevity of the device. Several attempts including the use of non-polar[7–13] substrates are being tried with varying degree of success. In the present article, we have reported yet unexplored potential of cuprous halides semiconductors for highly efficient LEDs. Our predictions agree with recent experimental results[39] at least qualitatively. Expected high performance of cuprous halides system is due to large exciton binding energy, vanishing electrostatic field in the active layer and close lattice match with the substrate, silicon. Considering that the application of cuprous halides semiconductors to optoelectronic devices is still in very early stage of research and development, we expect that our results reported in this article may have significant impacts on the future optoelectronic device technologies.

References

1. Ponce, F. A. & Bour, D. P. Nitride-based semiconductors for blue and green light-emitting devices. *Nature* **386,** 351–359 (1997).
2. Khan, M. A. *et al.* Lattice and energy band engineering in AlInGaN/GaN heterostructures. *Appl. Phys. Lett.* **43,** 1161–1163 (2000).
3. Bernardini, F., Fiorentini, V. & Vanderbilt, D. Spontaneous polarization and piezoelectric constants of III-V nitrides. *Phys. Rev. B* **56,** R10024–R10027 (1997).
4. Leroux, M. *et al.* Quantum confined Stark effect due to built-in internal polarization fields in (Al, Ga)N/GaN quantum wells. *Phys. Rev. B* **58,** R13371–R13374 (1998).
5. Park, S.-H. & Chuang, S. L. Piezoelectric effects on electrical and optical properties of wurtzite GaN/AlGaN quantum well lasers. *Appl. Phys. Lett.* **72,** 3103–3105 (1998).
6. Park, S.-H., Chuang, S. L. & Ahn, D. Piezoelectric effects on many-body optical gain of zinc-blend and wurtzite GaN/AlGaN quantum well lasers. *Appl. Phys. Lett.* **75,** 1354–1356 (1999).
7. Waltereit, P. *et al.* Nitride semiconductors free of electrostatic fields for efficient white light-emitting diodes. *Nature* **406,** 865–868 (2000).
8. Park, S.-H. & Chuang, S. L. Crystal-orientation effects on the piezoelectric field and electronic properties of strained wurtzite semiconductors. *Phys. Rev. B* **59,** 4725–4737 (1999).
9. Ng, H. M. Molecular-beam epitaxy of GaN/$Al_xGa_{1-x}N$ multiple quantum wells on R-plane $(10\bar{1}2)$ sapphire substrates. *Appl. Phys. Lett.* **80,** 4369–4371 (2002).
10. Chakaraborty, A. *et al.* Nonpolar InGaN/GaN emitters on reduced-defect lateral epitaxially overgrown a-plane GaN with drive-current-independent electroluminescence emission peak. *Appl. Phys. Lett.* **85,** 5143–5145 (2004).
11. Park, S.-H. Effect of $(10\bar{1}0)$ crystal orientation on many-body optical gain of wurtzite InGaN/GaN quantum well. *J. Appl. Phys.* **93,** 9665–9668 (2003).
12. Sharma, R. *et al.* Demonstration of a semipolar $(10\overline{1}\overline{3})$ InGaN/GaN green light emitting diode. *Appl. Phys. Lett.* **87,** 231110 (2005).
13. Ahn, D. & Park, S.-H. Theory of non-polar and semi-polar nitride semiconductor quantum-well structures. *Semicond. Science Technol.* **27,** 024001 (2012).
14. Makino, T. *et al.* Radiative recombinatiob of electron-hole pairs spatially separated due to quantum-confined Stark and Franz-Keldish effects in $ZnO/Mg_{0.27}Zn_{0.73}O$ quantum well. *Appl. Phys. Lett.* **81,** 2355–2357 (2002).
15. Gruber, Th., Kirchner, C., Kling, R. & Reuss, F. ZnMgO epilayers and ZnO-ZnMgO quantum wells for optoeletronic applications in the blue and UV spectral region. *Appl. Phys. Lett.* **84,** 5359–5361 (2004).
16. Park, S.-H. & Ahn, D. Spontaneous and piezoelectric polarization effects in wurtzite ZnO/MgZnO quantum wll lasers. *Appl. Phys. Lett.* **87,** 253509 (2005).
17. Look, D. C. & Claflin, B. P-type doping and devices based on ZnO. *Phys. Stat. Sol. (b)* **241,** 624–630 (2004).
18. Be'aur, L. *et al.* Exciton radiative properties in nonpolar homoepitaxial ZnO/(Zn, Mg)O quantum wells. *Phys. Rev. B* **84,** 165312 (2011).
19. Haug, H. & Jauho, A.-P. *Quantum Kinetics in Transport and Optics of Semiconductors*. (Springer-Verlag, Berlin, 1996, Germany).
20. Hanson, R. C., Haliberg, J. R. & Schwab, C. Elastic and piezoelectric constant of the cuprous halides. *Appl. Phys. Lett.* **21,** 490–492 (1972).
21. Williams, R. S., Shuh, D. K. & Segawa, Y. Growth and luminescence spectroscopy of a CuCl quantum well structure. *J. Vac. Soc. Technol. A* **6,** 1950–1952 (1987).
22. Masumoto, Y., Kawamura, T. & Era, K. Biexciton lasing in CuCl quantum dots. *Appl. Phys. Lett.* **62,** 225–227 (1993).
23. Nishida, N., Saiki, K. & Koma, A. Hetroepitaxy of CuCl on GaAs and Si substrates. *Surf. Sci.* **324,** 149–158 (1995).
24. Kawazoe, T. & Masumoto, Y. Luminescence hole burning and quantum size effect of charged excitons in CuCl quantum dots. *Phys. Rev. Lett.* **77,** 4942–4945 (1996).
25. Valenta, J., Moniatte, J., Gilliot, P., Honerlage, B. & Ekimov, A. I. Hole-filling of persistent spectral holes in the excitonic absorption band of CuBr quantum dots. *Appl. Phys. Lett.* **70,** 680–682 (1997).
26. Nakayama, M., Ichida, H. & Nishimura, H. Bound-biexciton photoluminescence in CuCl thin films grown by vacuum deposition. *J. Phys.: Condens. Matter* **11,** 7653–7662 (1999).
27. Goldmann, A., Tejeda, J., Shevchik, N. J. & Cardona, M. Density of valence states of CuCl, CuBr, CuI, and AgI. *Phys. Rev. B* **10,** 4388–4402 (1974).
28. Kleinman, L. & Mednick, K. Energy bands and effective masses of CuCl. *Phys. Rev. B* **20,** 2487–2490 (1979).
29. Ferhat, M., Zaoui, A., Certier, M., Dufour, J. P. & Khelifa, B. Electronic structure of the copper halides CuCl, CuBr and CuI. *Materials Sci. Eng.* **B39,** 95–100 (1996).
30. Ferhat, M., Bouhafs, B., Aourag, A., Zaoui, A. & Certier, M. The electronic structure of CuCl. *Comp. Materials Sci.* **20,** 267–274 (2001).
31. Valenta, J., Dian, J., Gilliot, P. & Honerlage, B. Photoluminescence and optical gain in CuBr semiconductor nanocrystals. *Phys. Stat. Sol. (b)* **224,** 313–317 (2001).
32. Gogolin, O. *et al.* Temperature dependence of exciton prak energies in CuI quantum dots. *Solid State Comm.* **122,** 511–512 (2002).
33. Gogolin, O. *et al.* Spectroscopically detected size-dependent temperature effects in I-VII compound nanocrystals: phase transitions and shift of the exciton peak energies. *J. Luminescence* **102,** 451–454 (2004).
34. Hwang, L. C. *et al.* Photoluminescence of I-VII semiconductor compounds. Sensitized luminescence from "deep states" recombination in CuBr/AgBr nanocrystals. *J. Chinese Chem. Soc.* **53,** 1235–1241 (2006).
35. O'Reilly, L. *et al.* Growth and characterization of wide-bandgap I-VII optoelectronc materials on silicon. *J. Materials Sci. : Materials in Electron.* **16,** 415–419 (2005).
36. O'Reilly, L. *et al.* Room-temperature ultraviolet luminescence from γ-CuCl grown near lattice-matched silicon. *J. Appl. Phys.* **98,** 113512 (2005).
37. O'Reilly, L. *et al.* Impact on structural, optical and electrical properties of CuCl by incorporation of Zn for n-type doping. *J. Cryst. Growth* **287,** 139–144 (2006).
38. Mitra, A. *et al.* Towards the fabrication of a UV light source based on CuCl thim films. *J. Mater. Sci.: Mater Electron* **18,** S21–S23 (2007),
39. Cowley, A. *et al.* UV emission on a Si substrate: Optical and structural properties of γ-CuCl on Si grown using liquid phase epitaxy techniques. *Phys. Stat. Sol. A* **206,** 923–926 (2009).

40. Cowley, A. *et al.* Electroluminescence of γ-CuBr thin films via vacuum evaporation deposition. *J. Phys. D.* **43,** 165101 (2010).
41. Ahn, D. & Chuang, S. L. High optical gain of I-VII semiconducgtor quantum wells for efficient light-emitting devices. *Appl. Phys. Lett.* **102,** 121114 (2013).
42. Knauth, R., Massiani, M. & Pasquinelli, M. Semiconductor properties of polycrystalline CuBr by Hall effect and capacitve measurements. *Phys. Stat. Sol. (a)* **165,** 461–645 (1998).
43. Danieluk, D. *et al.* Optical properties of undoped and oxygen doped CuCl films on silicon substrates. *J. Mater. Sci.: Mater. Electron.* **20,** S76–S80 (2009).
44. Grundmann, M *et al.* Cuprous iodide- a p-type transparent semiconductor: history and novel applications, *Phys. Stat. Sol. A* **210,** 1671–1703 (2013).
45. Brandt. O in *Group III nitride Semiconductor Compounds: Physics and Applications* (ed. Gil, B.) 417–459 (Oxford University Press, 1998).
46. Madelung, O. *Semiconductors: Data Handbook*. (Springer-Verlag, Berlin, 2004, Germany).
47. Bernardini, F. & Fiorentini, V. Spontaneous Polarization and Piezoelectric Constants of III-V Nitrides. *Phys. Rev.* **B56,** R10024–R10027 (1997).
48. Lawaetz, P. Valence-band parameters in cubic semiconductors. *Phys. Rev. B* **4,** 3460–3467 (1971).
49. Ahn, D. Optical gain of InGaP and cubic GaN quantum-well lasers with very strong spin-orbit coupling. *J. Appl. Phys.* **79,** 7731–7737 (1996).
50. Chao, C. Y.-P. & Chuang, S. L. Spin-orbit-coupling effects on the valence-band structure of strained semiconductor quantum wells. *Phys. Rev. B* **46,** 4110–4122 (1992).
51. Chuang, S. L. & Chang, C. S. Effective-mass Hamiltonian for strained wurtzite GaN and analytic solutions. *Appl. Phys. Lett.* **68,** 1657–1659 (1996).
52. Ahn, D. Theory of non-Markovian gain in quantum-well lasers. *Prog. Quant. Elecr.* **21,** 249–287 (1997).
53. Ahn, D. Theory of non-Markovian gain in strained-layer quantum-well lasers with many-body effects. *IEEE J. Quantum Electron.* **34,** 344–352 (1998).
54. Feezell, D. *et al.* Optical properties of nonpolar III-nitrides for intersubband photodetectors. *J. Appl. Phys.* **113,** 133103 (2013).
55. Van Roosebroeck, W. & Shockley, W. Photon-radiative recombination of electrons and holes in Germanium. *Phys. Rev.* **94,** 1558–1560 (1954).
56. Chuang, S. L., O'Gorman, J. & Levi, A. F. J. Amplified spontaneous emission and carrier pinning in laser diodes. *IEEE J. Quantum Electron.* **29,** 1631–1639 (1993).
57. Ahn, D. *et al.* Non-Markovian gain and luminescence of an InGaN-AlInGaN quantum-well with many-body effects. *IEEE J. Quantum Electron.* **41,** 1252–1259 (2005).
58. Bhattacharya, R., Pal, B. & Bansai, B. On conversion of luminesce into absorption and the van Roosbroeck-Shockley relation. *Appl. Phys. Lett.* **100,** 222103 (2012).
59. Goldmann, A. *et al.* Density of valence states of CuCl, CuBr, CuI, and AgI. *Phys. Rev. B* **10,** 4388–4402 (1974).

Acknowledgements

This work was supported by the 2015 Research Grant from the University of Seoul. The authors thank the late Professor Shun Lien Chuang for his insight as well as helpful discussions and dedicate this work to him.

Author Contributions

D.A. developed the theoretical construct and wrote the main manuscript and S.H.P. developed the numerical method for band-structure calculations. All authors reviewed the manuscript.

Additional Information

Competing financial interests: The authors declare no competing financial interests.

How to cite this article: Ahn, D. and Park, S.-H. Cuprous halides semiconductors as a new means for highly efficient light-emitting diodes. *Sci. Rep.* **6**, 20718; doi: 10.1038/srep20718 (2016).

This work is licensed under a Creative Commons Attribution 4.0 International License. The images or other third party material in this article are included in the article's Creative Commons license, unless indicated otherwise in the credit line; if the material is not included under the Creative Commons license, users will need to obtain permission from the license holder to reproduce the material. To view a copy of this license, visit http://creativecommons.org/licenses/by/4.0/